Dune orientation controlled by estuarine circulation in the Outer Weser estuary, German Bight, North Sea

M. Becker *Institute of Geosciences, CAU Kiel, Germany – marius.becker@ifg.uni-kiel.de*

G. Herrling *LKN, State Agency for Coastal Defense, National Park and Marine Conservation, Schleswig-Holstein, Kiel, Germany – gerald.herrling@lkn.landsh.de*

K. Krämer *Institute of Geosciences, CAU Kiel, Germany – knut.krämer@ifg.uni-kiel.de*

A. Lefebvre *MARUM, Center for Marine Environmental Sciences, University of Bremen, Germany – alefebvre@marum.de*

A. Zorndt *BAW, Federal Waterways Engineering & Research Institute, Hamburg, Germany – anna.zorndt@baw.de*

F. Kösters *BAW, Federal Waterways Engineering & Research Institute, Hamburg, Germany – frank.koesters@baw.de*

C. Winter *Institute of Geosciences, CAU, Kiel, Germany – christian.winter@ifg.uni-kiel.de*

ABSTRACT: Several years of monthly bathymetric surveys in the Weser estuary, Germany, show how the local effect of discharge on dune shape and orientation varies along the estuarine channel. Upstream located dunes are flood oriented during low discharge and ebb oriented during high discharge. The opposite is observed in the outer estuary during high discharge conditions, despite an increase of the depth-averaged ebb current velocity all along the channel. Model results suggest that this behavior is due to discharge related changes of the salt intrusion, and the related displacement of the brackish zone. During high discharge, estuarine circulation then alters the velocity structure in the outer estuary, then changing the bed load transport balance and dune orientation.

1 INTRODUCTION

While the emergence and migration of subaqueous dunes in unidirectional flow are well understood, much less is known about the dynamics of tidal dunes. This is especially the case for estuarine systems, where the velocity structure is complicated by baroclinic processes and asymmetries in mean tidal flow velocities.

For example, Hendershot et al. (2016) studied the shape of low-angle dunes on the tidal timescale, looking specifically at lee side angles and bedform height. On a longer timescale, Prokicki et al. (2022) found dune orientation to change in response to a displacement of the fluvial-tidal transition zone in the Lower Columbia River, US, during low discharge conditions. Lefebvre et al. (2021) described significant seasonal changes of steep slip face angles in the lower reaches of the Weser estuary. They indicated that discharge has an impact on dune asymmetry also in the outer estuary and suggested to explore the underlying mechanisms.

The Weser estuary does not exhibit a tidal-fluvial transition zone but is characterized by increasing tidal range from roughly 2.5 m in the outer estuary to more than 4 m at the weir. The weir is located 10 km upstream of river km 0, as used in the figures below. See Lefebvre et al. (2021) for a more detailed description of the dune distribution along the estuary.

2 DUNE PARAMETER EXTRACTION

Parameters describing the dune shape were determined based on an extensive bathymetric data set, acquired approximately every month by the local waterway and shipping administration (WSV).

Available data cover the years from 2008 to 2018. Altogether, 2190 grid files were provided and processed. The spatial resolution is 2 x 2 m. To generate bed elevation profiles (BEPs) grids were interpolated along the thalweg and along several profiles parallel to the thalweg. The lateral distance between the parallel profiles is 10 m. The number of profiles was defined to laterally cover the measured across-channel width.

Dunes in BEPs were identified by zero up and down crossing, roughly following Van der Mark et al. 2008. Bed elevations fluctuations smaller than 10 m were removed applying an appropriate low pass filter. A length scale of 250 m was used for detrending. Dune height was calculated as the distance of the crest to a straight line connecting the two troughs. Not all trough-crest-trough successions represent valid bedforms. Those are removed, using only feature heights between 0.3 m and 5 m, feature length between 15 m and 250 m, and a height to length ration between 0.01 and 0.2.

These steps work well for regular dunes. In case of irregular dunes, not all shapes are favorably detected and the zero crossing method introduced some typical cases of misidentified dunes, e.g. those with two local elevation maxima closer to the crest, or superimposed dunes. It is assumed that the use of parallel BEPs and the depiction of the same dune by several instances leads to statistically representative dune dimensions and directions.

Each grid is then associated with the date of acquisition, and each dune retrieved from BEPs is associated with an along-channel location in terms of river km. It occurred that the same location was measured twice with only a few days in between the two measurements, often as a result of overlaps between adjacent areas to be mapped, which could not be covered on the same day. Then, some locations were not measured for several weeks or even months, generating gaps in the presumably monthly time series for each location. Choosing a time interval of roughly one week (quarter month) combines data collected closely in time, but preserves the mentioned gaps, which allows specific treatment of these in the subsequent analysis.

Gaps in bathymetric data also exist spatially, in along-channel direction, meaning that at a certain point in time not all locations along the estuary were measured. Mean or median dune parameters were determined using an along-channel distance of 500 m. This steps still preserves the spatial variability of dune shape on the estuarine scale, but also preserves gaps, which can then be specifically treated in the analysis, such as for gaps in time.

Since each individual dune may be represented by many of the parallel BEPs, a minimum number of 250 values per 500 m was defined in order to determine median or mean dune parameters. In case of a channel width of 250 m, 25 parallel BEPs are processed.

If dunes crests reach across the entire channel, the same dune is found in all lines, and a minimum of 10 dunes must be located along the 500 m river stretch. Dunes in the Weser are irregularly distributed. Smaller dunes are abundant and should not be neglected in the analysis. As a result, the threshold of 250 values yields along-channel intervals to exhibit dunes, which are not typical dune fields, but may only contain a stretch of smaller dunes at the side of the navigation channel.

3 DUNE ORIENTATION

Here, changes in dune shape are more important than changes in length and height. This is because dune asymmetry is related to the respective face angles, certainly depending on the direction of net bedload transport and therefore on the regime of the tidal flow, often characterized as ebb or flood dominant by basic features of the tidal flow, such as depth averaged or peak ebb and flood velocities.

The spatial and temporal variability in dune asymmetry is shown in Figure 1. Asymmetry is given in terms of the face length asymmetry, which is the ratio between upstream and downstream face length. A remarkable number of dunes is in fact more symmetric than ebb-directed, as originally expected, especially in the regions up to km 10 and between km 55 and 105.
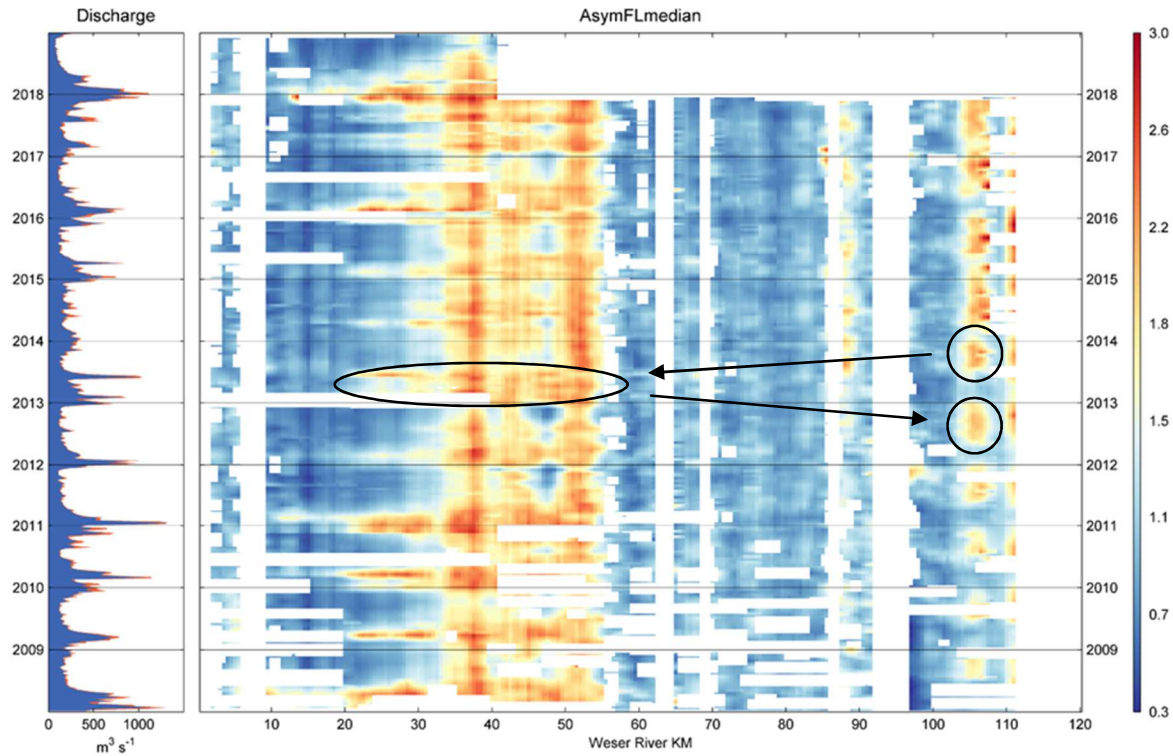
Figure 1. Median face length asymmetry in relation to discharge. Values are given in terms of the ratio of upstream versus downstream face length (FL). Symmetrical dunes exhibit a value of 1. Values exceeding 1 are ebb-directed. Encircled are examples of the occurrence of more flood directed dunes. River km increase downstream.
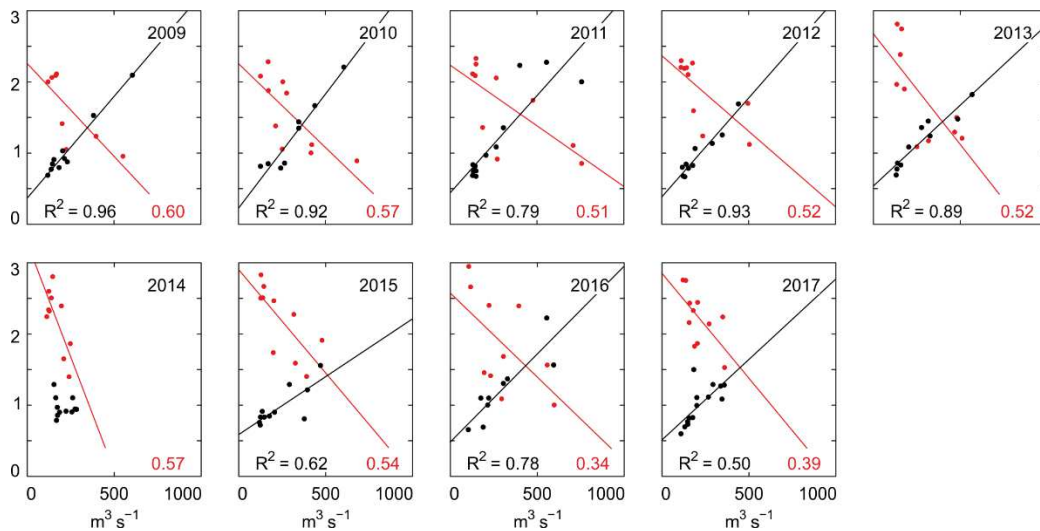

Figure 2. Face length asymmetry versus discharge, for each hydraulic year. Discharge is averaged for four weeks preceding the date associated with each data point of face length asymmetry. Results from km 25 (km 106) are shown in black (red). The typical discharge peak is missing in 2014, and dunes in the inner estuary are predominantly symmetric throughout the year. Note that no correlation line is given for km 25.

Mainly flood directed dunes are found between km 10 to 20. In the region between km 20 and 35, changes in dune asymmetry are related to discharge peaks, causing a change from symmetric or flood-directed to ebb-directed shapes. The opposite behavior is found e.g. around km 107, where dunes develop an ebb-directed shape during periods of

11

low discharge. The response of dune shape to discharge variations therefore depends on the location within the estuary. Such spatial variations of dune shape response are expected to occur in a funnel-shaped, partially-mixed estuary with a strong barotropic tide. The tidal asymmetry might vary along the channel and in time, and it is presumed, as said, that dune shape reflects the effect of that tidal asymmetry on residual bed load transport.

Dune parameter and discharge are correlated for each hydraulic year separately. Figure 2 shows an example of two different along-channel locations. The slope of the corresponding linear regression is a first estimation of the dune response to discharge variations, neglecting lag effects.

The correlation coefficient in Figure 2 is consistently higher in the inner compared to the outer estuary, indicating the control of discharge on dune asymmetry to decrease downstream. Regression slopes determined for different hydraulic years are interpreted as the response of a parameter to change with discharge and averaged at each location. The regressions show the oppositional behavior of dune asymmetry in the inner and in the outer estuary.

Clearly, low discharge causes dunes to develop flood-directed shapes in the inner and ebb-directed shapes in the outer estuary. The contrary seems to occur during high discharge conditions. It remains to determine in which particular way hydrodynamics change in response to high discharge in the outer estuary.

4 HYDRODYNAMIC MODEL

The analysis of changes of the velocity structure in response to discharge is based on results from a 3D numerical model (UN-TRIM2, BAW). The simulation period is from 2019 May to 2020 April. Model results are available for 16 cross-sections, located along the channel between km 30 and km 105, in along-channel steps of approximately 5 km. The vertical resolution is 0.5 m. Across-channel horizontal resolution and corresponding mesh cell size are variable. The number of across-channel mesh cells ranges from 8 (far upstream) to 52 (outer estuary).

The model was validated with respect to variations of the salt intrusion and the vertical density stratification, based on ship-based measurements during the simulation period and data from several stations of salinity, distributed along the estuary. Parameters used here, as obtained from model results, are the near-bed residual velocity, the salt flux, stratification, and the tidal velocity asymmetry.

The near-bed residual velocity was determined as the minimum value of the residual velocity profile. This profile is based on tidal velocities projected with respect to the ebb current direction. A negative, upstream-directed near-bed velocity should indicate an estuarine exchange flow to effect the residual velocity profile, probably somewhere along the brackish zone.

The salt flux was decomposed using the flux decomposition method of Becherer et al. (2016), there used to decompose fluxes of suspended sediment, here applied to salinity. To perform the decomposition, salinity and velocity were interpolated vertically on a sigma grid and corrected for the tidally varying vertical layer spacing, to preserve continuity of the flux. The decomposition then splits the subtidal or net salt flux into three components, taking into account intratidal variations of the vertical profiles of current velocity and salinity.

It is arguable if the salt flux components, resulting from this decomposition, can be addressed as to represent the influences of distinct mechanisms, which would be the tidal pumping flux, the barotropic flux, and the contribution due to exchange flow (Becherer et al. 2016). These flux components have been addressed differently across literature (e.g. Geyer et al. 2001, Burchard et al. 2017, Dijkstra et al. 2022). Here only the contribution due to the exchange flow is used.

Stratification is quantified by the potential energy anomaly (Simpson et al. 1978, Burchard and Hofmeister 2008), as determined from the vertical density distribution and subsequently used to show variations of stratification in response to changes of discharge.
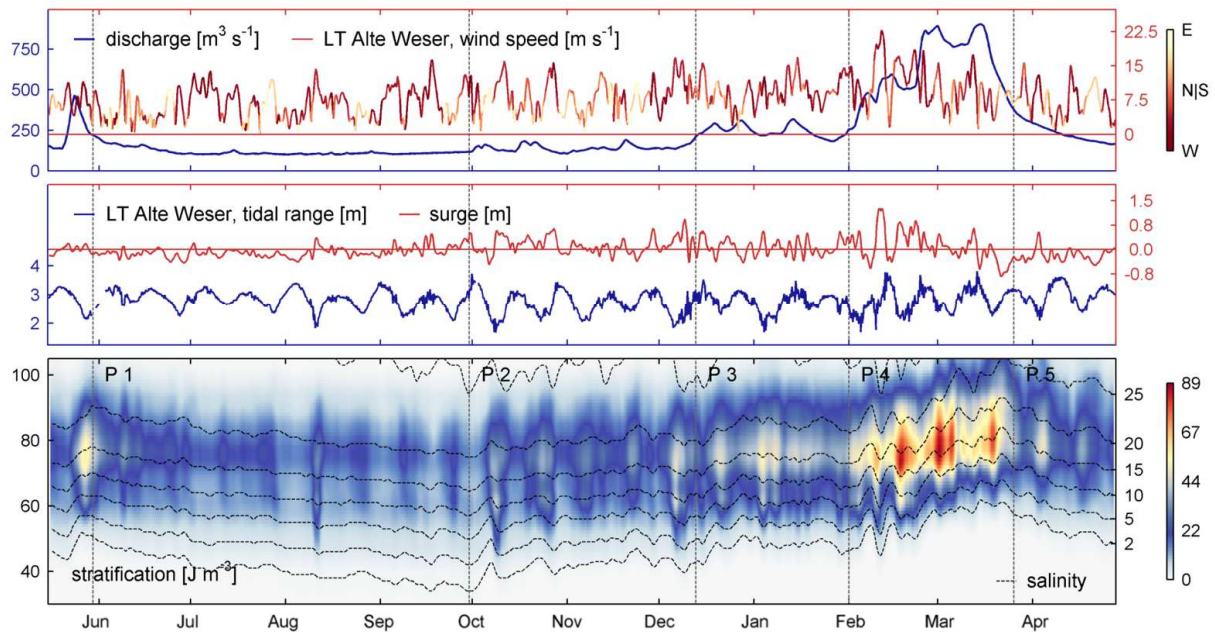
Figure 3. Stratification, discharge, tidal range, wind, and surge during the simulation period. Stratification is plotted in terms of the potential energy anomaly. In the top panel, wind speed is color coded with respect to wind direction, red colors indicate westerly winds. The surge was determined by harmonic analysis, subtracting the reconstructed tidal signal from the measured elevation (Pawlowicz, 2002). Wind and water level elevation (tidal range) are as measured in the Outer Weser, at lighthouse (LT) Alte Weser. Salinity at isohalines is indicated by y-axis labels on the right side of the bottom panel. X-axis labels indicate river km.
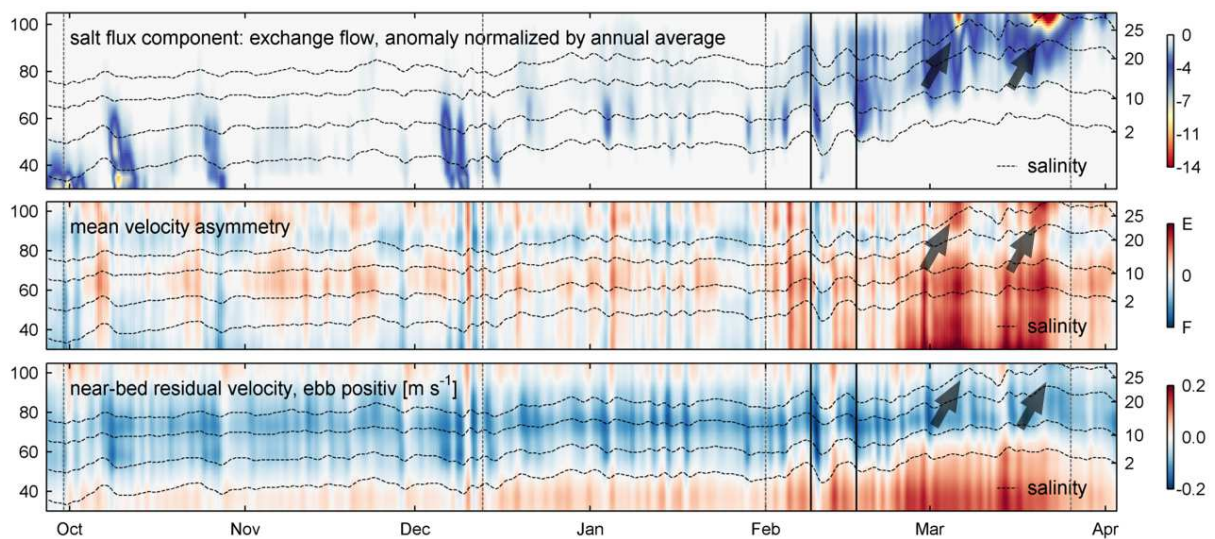

Figure 4. Salt flux due to exchange flow, velocity asymmetry and near-bed velocity between the periods P2 and P4. See text and Figure 3 for explanation of the periods. The exchange flow component of the salt flux is given as its deviation from the annual average, normalized by that annual average. To show the along-channel variations during the simulation period, the annual average and the respective deviations are determined for each location along the river. Arrows point to two distinct discharge peaks during P4. Black vertical lines indicate two storm surges, which affected water levels in the German Bight and occurred during the main increase of discharge.

The tidal velocity asymmetry was calculated as follows. For each tidal phase the velocity was depth and cross-sectionally averaged, in the same flux-preserving way along sigma layers as applied to determine salt flux components. The average ebb velocity was then related to the sum of the ebb and flood velocity, which yields an asymmetry estimate around the value of 0.5. Values exceeding 0.5 indicate ebb velocity dominance

Figure 3 shows the salt intrusion and stratification along the variations of environmental conditions during the simulation period. Stratification is based on the along-channel profile and averaged over two tidal cycles. Isohalines indicate how the salt intrusion changes on various time scales, mainly in response to changes of the discharge.

5 DISCHARGE AND CIRCULATION

The time series is split into periods, each characterized by a certain stratification, discharge and salt intrusion. The maximum of stratification is located around river km 70 during low discharge. Stratification increases during neap tides, certainly in response to lower than average tidal current velocities and less mixing. Stratification increases significantly during times of high discharge in March 2020, during P4 and P5. Then, the salt intrusion decreases and the brackish zone is displaced further downstream, such as the location of maximum stratification.

Figure 4 presents evidence for the change of the vertical velocity structure in the outer estuary, which occurs in response to the increased discharge. While the mean velocity asymmetry indicates increased ebb-dominance, the near-bed velocity is flood-directed, downstream of km 85. In addition, the effect of the exchange flow on the salt flux increases substantially in the outer estuary, especially during the two discharge peaks. The implications are discussed, as follows.

6 DISCUSSION

To start it is noted that the mean velocity asymmetry downstream of km 85 does not reflect the velocity structure close to bed, and cannot be interpreted as to indicate any favorable direction of bed sediment transport. The deviation between the dominant directions inferred from the velocity asymmetry and the near-bed residual current are due to the nature of the estuarine tidal shear flow, which is shown to effect also the salt flux, by the exchange flow component. Here it is not analyzed, which particular process would then be responsible for the changes of the residual flow profile. Processes involved are complex and their understanding underwent substantial corrections in the past decades (e.g. Dijkstra et al. 2020).

However, results show a spatial correlation between the along-channel location of the salt intrusion and stratification on one hand, and the change of the velocity structure on the other hand. Note that also the maximum along-channel density gradient is displaced downstream, accordingly. This indicates that the exchange flow profile, emerging in the outer estuary during high discharge, is controlled by processes related to and driven by the estuarine along-channel and vertical density structure, e.g. by the subtidal, gravitational circulation, by tidal straining and by associated tidal asymmetries in stratification and mixing.

The reversal of dune orientation requires at least a change of the bed load transport balance. Certainly, this change would be induced by the altered direction of the near-bed residual velocity, as it is found in model results during high discharge conditions.

Both the reversal of dune orientation as well as the change of the near-bed velocity occur downstream of km 85. It is concluded that effects due to estuarine circulation, or rather the displacement of its effective location, determine the shape of dunes in the outer Weser estuary. Similar conclusions were drawn by Berne et al. (1993) for the Gironde estuary, who suggested that the migration direction of large dunes was influenced by estuarine circulation. Following up on the Gironde case, van der Sande et al. (2021) applied an analytical model of estuarine flow and linear stability analysis, diagnostically imposing an along-channel salinity gradient, which introduced the development of gravitational circulation in their model. There, a relatively low

eddy viscosity and low river flow was required to induce upstream dune migration. They, however, note that the migration direction of dunes was not necessarily the same as the direction of net sediment transport. In that sense, several aspects remain to be explored. The simulated bed shear stress and bed load sediment transport have not been analyzed, such as along-channel variations of the properties of bed sediments. Lateral processes affecting the along-channel velocity structure were neglected. Lag-effects between discharge, the salt intrusion and changes in dune shape were not considered.

Here is to say that data processed for this study show no indications for week-long lags as reported by Allen (1976), who revisited data acquired by Nasner (1974) in the Weser estuary. It is expected that bed load transport responds relatively quickly to a change in discharge and the corresponding change in current velocity.

How the new bed load transport then leads to a change in dune asymmetry and ultimately in dune direction depends on the pre-existing dune shape. This defines the mass of sediment required to be transported, which is essentially Allen's "intrinsic resistance of individual bedforms to any kind of change". Note that in case of the Weser, all measured discharge peaks must have sufficiently altered the transport balance, as they all induced changes in dune asymmetry, not only in the Outer Weser, but all along the estuarine channel.

7 REFERENCES

Allen, J. R. L., 1976. Time-lag of dunes in unsteady flows: An analysis of Nasner's data from the River Weser, Germany. Sedimentary Geology, 15(4), 309-321

Becherer, J., Flöser, G., Umlauf, L., Burchard, H., 2016. Estuarine circulation versus tidal pumping: Sediment transport in a well-mixed tidal inlet. Journal of Geophysical Research: Oceans, 121(8), 6251-6270

Becker, M., Schrottke, K., Bartholomä, A., Ernstsen, V., Winter, C., Hebbeln, D., 2013. Formation and entrainment of fluid mud layers in troughs of subtidal dunes in an estuarine turbidity zone. Journal of Geophysical Research: Oceans, 118(4), 2175-2187

Berne, S., Castaing, P., Le Drezen, E., Lericolais, G., 1993. Morphology, internal structure, and reversal of asymmetry of large subtidal dunes in the entrance to Gironde Estuary (France). Journal of Sedimentary Research, 63(5), 780-793

Burchard, H., Hofmeister, R., 2008. A dynamic equation for the potential energy anomaly for analysing mixing and stratification in estuaries and coastal seas. Estuarine, Coastal and Shelf Science, 77(4), 679-68

Burchard, H., Schuttelaars, H.M., Ralston, D.K., 2017. Sediment Trapping in Estuaries. Annual Review of Marine Science

Dijkstra, Y. M., Schuttelaars, H. M., Kranenburg, W. M., 2022. Salt Transport Regimes Caused by Tidal and Subtidal Processes in Narrow Estuaries. Journal of Geophysical Research: Oceans, 127(12)

Geyer, W. R., Woodruff, J. D., Traykovski, P., 2001. Sediment transport and trapping in the Hudson River estuary. Estuaries and Coasts, 24(5), 670-679.

Geyer, W. R., MacCready P., 2014. The Estuarine Circulation. Annual Review of Fluid Mechanics, 46(1), 175-197

Hendershot, M. L., Venditti, J. G., Bradley, R. W., Kostaschuk, R. A., Church, M., Allison, M. A., 2016. Response of low-angle dunes to variable flow. Sedimentology, 63(3), 743-760

Lefebvre, A., Herrling, G., Becker, M., Zorndt, A., Krämer, K., Winter, C., 2022. Morphology of estuarine bedforms, Weser Estuary, Germany. Earth Surface Processes and Landforms, 47(1), 242-256

Nasner, H., 1974. Über das Verhalten von Transportkörpern im Tidegebiet. Mitteilungen des Franzius-Instituts für Wasserbau und Küsteningenieurwesen, 40, 1-140

Prokocki, E. W., Best, J. L. , Perillo, M. M. , Ashworth, P. J., Parsons, D. R., Sambrook Smith, G. H., Nicholas, A. P., Simpson, C. J., 2022. The morphology of fluvial-tidal dunes: Lower Columbia River, Oregon/Washington, USA. Earth Surface Processes and Landforms, 47(8), 2079-2106

Simpson, J. H., Allen, C. M., Morris, N. C. G., 1978. Fronts on the Continental Shelf. Journal of Geophysical Research, 83, 4607-4614

Van der Mark, C. F., Blom, A., Hulscher, S. J. M. H., 2008. Quantification of variability in bedform geometry. Journal of Geophysical Research, 113(F03020), 11

Van der Sande, W. M., Roos, P., C., Gerkema, T., Hulscher, S. J. M. H., 2021. Gravitational Circulation as Driver of Upstream Migration of Estuarine Sand Dunes. Geophysical Research Letters 48(14)